JACS
JOURNAL OF THE AMERICAN CHEMICAL SOCIETY

Communication

pubs.acs.org/JACS

Spectroscopic and Crystallographic Evidence for the Role of a Water-Containing H-Bond Network in Oxidase Activity of an Engineered Myoglobin

Igor D. Petrik,[†,§] Roman Davydov,[‡,§] Matthew Ross,[†,‡] Xuan Zhao,[†] Brian Hoffman,[*,‡] and Yi Lu[*,†]

[†]Department of Chemistry, University of Illinois at Urbana−Champaign, Urbana, Illinois 61801, United States

[‡]The Department of Chemistry, Northwestern University, Evanston, Illinois 60201, United States

Supporting Information

ABSTRACT: Heme-copper oxidases (HCOs) catalyze efficient reduction of oxygen to water in biological respiration. Despite progress in studying native enzymes and their models, the roles of non-covalent interactions in promoting this activity are still not well understood. Here we report EPR spectroscopic studies of cryoreduced oxy-F33Y-Cu_BMb, a functional model of HCOs engineered in myoglobin (Mb). We find that cryoreduction at 77 K of the O_2-bound form, trapped in the conformation of the parent oxyferrous form, displays a ferric-hydroperoxo EPR signal, in contrast to the cryoreduced oxy-wild-type (WT) Mb, which is unable to deliver a proton and shows a signal from the peroxo-ferric state. Crystallography of oxy-F33Y-Cu_BMb reveals an extensive H-bond network involving H_2O molecules, which is absent from oxy-WTMb. This H-bonding proton-delivery network is the key structural feature that transforms the reversible oxygen-binding protein, WTMb, into F33Y-Cu_BMb, an oxygen-activating enzyme that reduces O_2 to H_2O. These results provide direct evidence of the importance of H-bond networks involving H_2O in conferring enzymatic activity to a designed protein. Incorporating such extended H-bond networks in designing other metalloenzymes may allow us to confer and fine-tune their enzymatic activities.

Activation of O_2 is important in biology because O_2, despite its high abundance in the Earth's atmosphere and high oxidizing power, is kinetically inert. A prominent example of O_2 activation is aerobic respiration, in which the oxidizing potential of O_2 is used to generate a proton gradient, driving synthesis of adenosine triphosphate, the energy source for most biological processes. This reaction is efficiently catalyzed by terminal oxidases, e.g., heme-copper oxidases (HCOs) containing a heme and Cu_B center[1] and cytochrome (cyt) *bd*-oxygen reductases with only hemes at the active site.[2] While these enzymes and their model systems have been extensively studied and mechanisms have been proposed,[1−3] an understanding of structural features responsible for O_2 activation is still being sought. For example, while a number reports have elucidated H-bond networks in the channels *leading to* the Cu_B site in HCOs,[1,3a,b] experimental support for structural features, e.g., a putative H-bond network involving H_2O *within* the Cu_B site, proposed by computational modeling,[4] remains elusive.

To elucidate structural features responsible for efficient O_2 activation, biochemical and biophysical studies of the oxidases and related enzymes have identified potentially important amino acid residues in the reaction, which has been confirmed by loss of activity in site-directed mutagenesis (SDM) studies.[1,3a,b,5,6] However, these mutations often cause structural perturbations in addition to those directly being investigated, which may cause loss of function. Moreover, SDM studies reveal only necessary, but not minimally sufficient structural features for function. To overcome this limitation, synthetic models of native enzymes have been prepared, and their studies have offered deeper insights into the structural features responsible for oxidase activity.[3c,d,7]

As a complementary approach to the studies of native enzymes and their synthetic models, use of small designed metalloproteins and -peptides has shown remarkable success.[8] For example, we have employed a "biosynthetic modeling" approach, based on a small natural protein scaffold, to gain fundamental understanding of sufficient features conferring oxidase activity, i.e., $4e^-$ reduction of O_2 to H_2O.[8a,9] In contrast to native enzymes, such as HCOs, which are membrane proteins that are not easy to purify to homogeneity with high yields and contain other accessory metal sites that can complicate spectroscopic studies, biosynthetic models are simpler to synthesize and contain only the metal-binding site central to the enzymatic activity. While most HCO models use organic molecules as ligands, our biosynthetic approach uses small, stable, and well-characterized proteins, such as sperm whale myoglobin (Mb), as the scaffold. Thanks to recent advances in biology, biosynthetic models of complex metal-binding sites can be prepared more easily and with higher yields than using organic molecule ligands. Furthermore, the structurally rigid scaffold protein allows defining long-range non-covalent interactions and probing their roles more precisely. Using this approach, we previously reported the design of an HCO mimic by introducing two His and one Tyr residues in the active site of wild-type (WT) Mb (named F33Y-Cu_BMb) and found that, unlike WTMb, which only binds O_2 reversibly, this protein achieves O_2 reduction to H_2O with >500 turnovers.[9d] Thus, this minimal functional mimic, much simpler than native oxidases while still functioning under physiological conditions, provides a platform for elucidating structural features responsible for O_2 reduction that bridges the gap between native enzymes and small molecular mimics of native enzymes.

Received: November 16, 2015
Published: December 30, 2015

DOI: 10.1021/jacs.5b12004
J. Am. Chem. Soc. 2016, 138, 1134−1137

Scheme 1. Proposed Mechanism of O_2 Reduction by F33Y-Cu_BMb in Comparison with WTMb

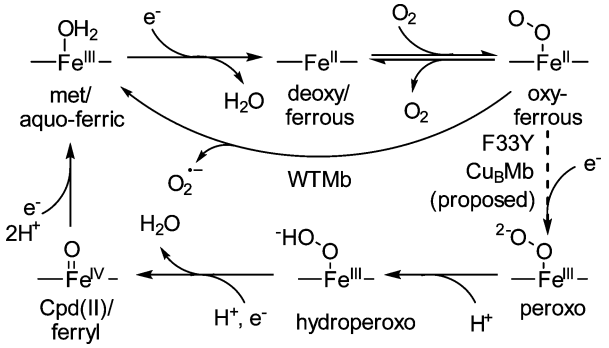

Scheme 2. Formation and Trapping of (Hydro)peroxo Intermediates by Cryoreduction

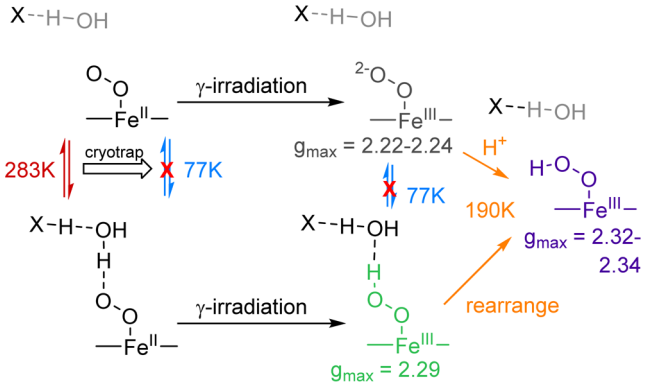

We hypothesize that F33Y-Cu_BMb operates by heterolytic O–O bond cleavage (Scheme 1), analogous to the accepted mechanism for native oxidases and monooxygenases, but the detailed structural features and interactions that promote this reaction in F33Y-Cu_BMb are still unclear. Here we use cryogenic EPR spectroscopy and high-resolution X-ray crystallography to show that an extensive H-bond network involving H_2O molecules exists in the active site of F33Y-Cu_BMb and plays an important role in facilitating proton delivery to the oxygen and activating it for reduction, thus, imparting oxidase activity.

EPR has been widely used to probe the environment of O_2-activating iron enzymes.[10] Although oxy-heme is an electronically closed-shell system with no EPR signal, EPR spectroscopy has been used to offer insight into the properties of oxy-heme, e.g., its interactions with nearby residues and its intermediates upon reduction, by a method called cryoreduction.[11] Briefly, the oxy-heme protein, trapped at 77 K, is exposed to γ-radiation, releasing "free" electrons into the sample matrix to efficiently reduce EPR-silent oxy-heme into EPR-active peroxo-heme. Because cryogenic trapping suppresses thermal relaxation and equilibration of the protein and its active site, EPR spectra of the resulting sample, maintained at 77 K, provide valuable structural information on the oxy-heme precursor (Scheme 2).[10a,f−l,11] Furthermore, the peroxo-heme products are intermediates along the pathway of O_2 reduction, and subsequent decay, achieved by stepwise warming of the samples, followed by rapid recooling to 77 K after each step to trap intermediates-a procedure called annealing, provides further insight into the reaction (Scheme 1).[10a,11,12] As a result, EPR spectroscopy in combination with cryoreduction and annealing has been used over the past two decades to probe the structure and interactions of O_2 in many heme proteins, including

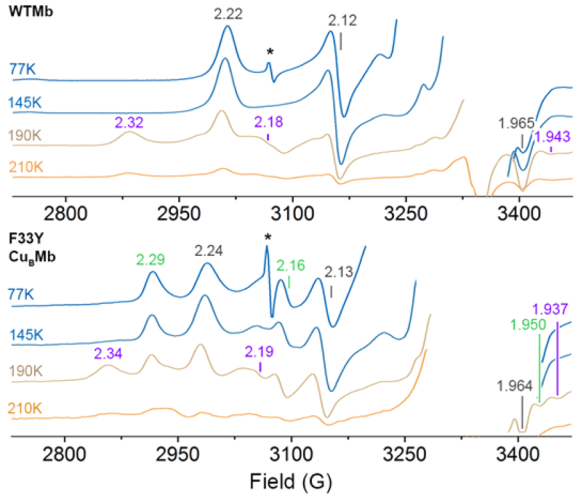

Figure 1. EPR spectra of oxy-WTMb and oxy-F33Y Cu_BMb after radiolytic reduction with a ~3 Mrad dose of γ radiation from ^{60}Co, and after subsequent stepwise annealing for 1 min at indicated temperatures (sharp signal marked by asterisk is due to radiolytically generated H-atoms at 77 K in quartz EPR tube).

Table 1. *g*-Values of Cryoreduced Oxy-ferrous Myoglobins

protein		g_1	g_2	g_3
WTMb	peroxo	2.22	2.12	1.965
	hydroperoxo[a]	2.32	2.18	1.943
F33y Cu_BMb	peroxo	2.24	2.13	1.964
	hydroperoxo[b]	2.29	2.16	1.950
	hydroperoxo[a]	2.34	2.19	1.937

[a]Hydroperoxo product formed upon annealing. [b]Primary hydroperoxo product formed at 77 K.

myoglobins and monooxygenases.[10a,f−o,11,12] Because WTMb, the scaffold for F33Y-Cu_BMb, was among the first and most studied proteins by the above method, the abundance of results facilitates understanding of the latter by direct comparison. In this study, F33Y-Cu_BMb contained heme but no metal ion in the Cu_B site, because a previous report showed that this protein exhibits high oxidase activity without a metal ion at Cu_B,[9d] mimicking cyt *bd*-oxygen reductases, which lack this site.[2]

Figure 1 shows EPR spectra of oxy-WTMb and oxy-F33Y-Cu_BMb cryoreduced at 77 K, obtained under the same conditions. The WTMb spectrum shows the signal from a single species with g = [2.22, 2.13, 1.96] (see Figure S1 for spectra at other temperatures) whose EPR parameters (Table 1) identify it as a ferric-peroxo state, with the peroxo ligand H-bonded to the distal His-64.[10f−i,11] In contrast, the cryoreduced oxy-F33Y-Cu_BMb exhibits two rhombic EPR signals (Figures 1, S1, and S2). The first, with g = [2.24, 2.13, 1.95], is similar to that of the ferric-peroxo species in WTMb. The second, more rhombic EPR signal, has g = [2.29, 2.17, 1.96], in the range characteristic of ferric-hydroperoxo intermediates.[10a,h,k−m] This assignment is supported by ^{1}H ENDOR measurements (Figure S6), where the g_{max} = 2.24 species has been removed by annealing, showing a maximum proton coupling of ~9.5 MHz. Ferric-peroxo intermediates show strongly coupled exchangeable proton signals with $A_{max} \approx 14–18$ MHz,[10a,i,n] while hydroperoxo- exhibit a smaller coupling, $A_{max} \leq 13$ MHz.[10j,k,o] The absence of signal with $A_{max} > 13$ MHz confirms that the more rhombic species observed in F33Y-Cu_BMb is hydroperoxo, not peroxo.

DOI: 10.1021/jacs.5b12004
J. Am. Chem. Soc. 2016, 138, 1134−1137

To gain further insight into O_2 reduction by F33Y-Cu_BMb, we monitored the decay of the above cryoreduced species by annealing. As previously reported, annealing the cryoreduced oxy-WTMb at 190 K converts the peroxo signal with g_{max} = 2.22 to the more rhombic EPR signal of a ferric-hydroperoxo intermediate, with g = [2.32, 2.18, 1.93] (Figures 1 and S1), through protonation of the peroxo moiety.[13] Upon annealing of cryoreduced oxy-F33Y-Cu_BMb at 173−175 K for at least 1 min, a signal with g = [2.34, 2.19, 1.94] begins to appear and continues to grow in at 190 K (Figures 1, S1, and S2). These EPR parameters are very similar to those of ferric-hydroperoxo-WTMb. Appearance of this signal during annealing is interpreted to arise from both protonation of the ferric-peroxo centers with g_{max} = 2.24 to form ferric-hydroperoxo, and relaxation/repositioning of the hydroperoxo ligand of the g_{max} = 2.29 species of the heme iron (Scheme 2).

Based on the known reactivity of the (hydro)peroxo-hemes, these intermediates are expected to thermally decompose to compound II (CpdII), a ferryl species that is EPR silent. Consistent with this expectation, further annealing both samples at 210 and 220 K (Figures 1 and S1) results in obvious decay of the (hydro)peroxo signals to an EPR-silent state. It has been shown that further cryoreduction of the EPR-silent CpdII (Fe(IV)=O^{2-}) at 77 K generates a low-spin rhombic EPR signal from the Fe(III)−O^{2-} or Fe(III)−OH^- species, depending on the protonation state of ferryl precursor. Subsequent cryoreduction of the EPR-silent species in WTMb resulted in a signal with g = [2.43, −, 1.93] (Figure S3), characteristic of Fe(III)−O^{2-} (ferric oxo) species observed in cryoreduced CpdII (g = [2.43, 2.12, 1.93]),[12c] confirming the EPR-silent state arising after annealing of (hydro)peroxo-WTMb as the Fe(IV)=O^{2-} CpdII. A minor signal with g = [2.52, −, 1.90] (Figure S3) was also observed, previously assigned as protonated ferric-oxo, i.e., ferric-hydroxo (Fe(III)−OH^-).[12c] In the case of F33Y-Cu_BMb, further cryoreduction of the EPR-silent annealed species yielded a dominant EPR signal with g = [2.52, 2.15, 1.90] (Figure S3), likewise assigned as ferric-hydroxo. This result supports the hypothesis that the hydroperoxo-F33Y-Cu_BMb converts to CpdII. This assignment is confirmed by comparison with the same signals observed in cryoreduced samples of CpdII, generated in both proteins by reaction with H_2O_2 at 21−25 °C (Figure S4).

Observation of two distinct signals in cryoreduced oxy-F33Y-Cu_BMb at 77 K suggests the presence of two structural states of the oxy-ferrous precursor. The peroxo signal with g_{max} = 2.24 is nearly identical to the signal observed in WTMb and well within the range of those of other oxygen-binding proteins such as hemoglobin,[10h,i] suggesting that the oxy-ferrous population leading to this state has similar interactions and behaves in a similar manner. On the other hand, the observation of a hydroperoxo species with g_{max} = 2.29 at 77 K requires a configuration in which the oxygen can be easily protonated at 77 K (Scheme 2). The observation of protonated Fe(III)−OH^- in F33Y-Cu_BMb upon subsequent cryoreduction of annealed species provides further support for the facile protonation of intermediates. Previous cryoreduction studies of a variety of oxy-heme proteins[10a,j−n,12a,b] showed that proton transfer to a cryoreduced oxy-heme at 77 K requires the presence of an extended H-bonded proton delivery network in the oxy-ferrous protein that includes protic residues and at least one ordered H_2O molecule H-bonded to the terminal O-atom of the O_2 ligand. Based on these observations, we hypothesized that the F33Y-Cu_BMb may contain a similar H-bond network for faster proton delivery to the oxy-heme than in WTMb. To test this, we obtained the crystal structure of oxy-F33Y-Cu_BMb.

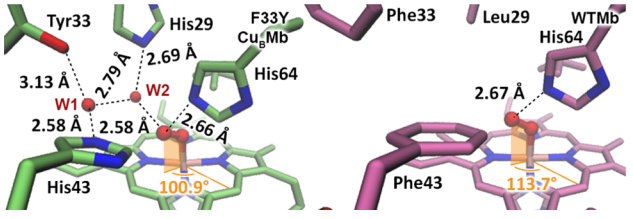

Figure 2. Crystal structure of oxy-F33Y-Cu_BMb determined at 1.27 Å resolution (PDB: 5HAV), compared with that of oxy-WTMb (1A6M).[16]

The oxy-F33Y-Cu_BMb crystal was prepared by soaking ferric-Mb crystals in dithionite, followed by exposure to O_2,[14] and the oxy state was confirmed by single-crystal UV/vis spectroscopy before diffraction (Figure S5). The structure, refined at 1.27 Å resolution, is compared with the structure of oxy-WTMb in Figure 2.[15] An omit-map showing the electron density of the oxygen ligand is shown in Figure S6. Due to reduced oxygen affinity of F33Y-Cu_BMb, refinement of this structure yielded an incomplete occupancy for the oxygen ligand, but it nevertheless supports the above interpretation of the EPR data. As suggested by the EPR results, an extended H-bond network involving two H_2O molecules is observed, with W1 stabilized by H-bonds with the engineered His43 and Tyr33 residues, and W2 stabilized by H-bonds to W1 and the engineered His29 (Figure 2). Together, this H-bond network links the designed residues and the distal O-atom of bound O−O. As a result of these changes in the active-site pocket, the O−O in F33Y-Cu_BMb is rotated from that in WTMb by ∼13° about the Fe−O bond, apparently to maximize its ability to accept H-bonds from His64 and W2. Such an interaction of the oxygen with the W2 is expected to enable the facile protonation, by W2, of the peroxo intermediate formed on cryoreduction at 77 K, yielding the hydroperoxo observed by the cryogenic EPR.

Given the spectroscopic and crystallographic evidence for an H-bond network that interacts with the O_2 in oxy-F33Y-Cu_BMb, and its absence in oxy-WTMb, we conclude that this H-bond network is the important structural feature that transforms WTMb, a protein that can only bind O_2 reversibly, into F33Y-Cu_BMb, a protein that can activate O_2 and reduce it to H_2O. We propose that this activation is achieved by polarization of the O−O bond by the H-bonded H_2O, allowing facile reduction and protonation of the oxygen and intermediates. While H-bond networks involving water have been observed in native heme enzymes such as cyt P450[10l,m,17] and a similar network has been proposed to occur in HCOs-based computational and isotope studies,[4] design of metalloenzymes incorporating this important structural feature has been difficult to perform and confirm. The combination of cryoreduction EPR spectroscopy and high-resolution crystallography presented in this work provides a clear example of the importance of H-bond networks involving water in conferring activity to designed metalloenzymes. We believe this structural feature will be critical to enhancing the future success of high-activity metalloenzyme design.

■ ASSOCIATED CONTENT

Supporting Information

The Supporting Information is available free of charge on the ACS Publications website at DOI: 10.1021/jacs.5b12004.

Methods, spectra, and crystallographic data (PDF)

DOI: 10.1021/jacs.5b12004
J. Am. Chem. Soc. 2016, 138, 1134−1137

AUTHOR INFORMATION

Corresponding Authors

*bmh@northwestern.edu

*yi-lu@illinois.edu

Author Contributions

§I.D.P. and R.D. contributed equally.

Notes

The authors declare no competing financial interest.

ACKNOWLEDGMENTS

We thank Dr. S. Toshkov for assistance with γ-irradiation, Drs. V. Šrajer and R. Henning for assistance with crystal studies at BioCARS, and Drs. P. Hosseinzadeh, S. Tian, and I. Denisov for helpful discussions. Research reported in this publication was supported by the National Institutes of Health (R01GM062211 to Y.L. and R01GM111097 to B.M.H.).

REFERENCES

(1) (a) Ferguson-Miller, S.; Babcock, G. T. *Chem. Rev.* **1996**, *96*, 2889. (b) Namslauer, A.; Brzezinski, P. *FEBS Lett.* **2004**, *567*, 103.

(2) Borisov, V. B.; Gennis, R. B.; Hemp, J.; Verkhovsky, M. I. *Biochim. Biophys. Acta* **2011**, *1807*, 1398.

(3) (a) Kaila, V. R. I.; Verkhovsky, M. I.; Wikström, M. *Chem. Rev.* **2010**, *110*, 7062. (b) Brzezinski, P.; Gennis, R. B. *J. Bioenerg. Biomembr.* **2008**, *40*, 521. (c) Collman, J. P.; Devaraj, N. K.; Decréau, R. A.; Yang, Y.; Yan, Y.-L.; Ebina, W.; Eberspacher, T. A.; Chidsey, C. E. D. *Science* **2007**, *315*, 1565. (d) Kim, E.; Chufán, E. E.; Kamaraj, K.; Karlin, K. D. *Chem. Rev.* **2004**, *104*, 1077.

(4) (a) Blomberg, M. R. A.; Siegbahn, P. E. M.; Wikström, M. *Inorg. Chem.* **2003**, *42*, 5231. (b) Cukier, R. I. *Biochim. Biophys. Acta* **2005**, *1706*, 134. (c) Proshlyakov, D. A.; Ogura, T.; Shinzawa-Itoh, K.; Yoshikawa, S.; Kitagawa, T. *Biochemistry* **1996**, *35*, 8580. (d) Yoshioka, Y.; Kawai, H.; Yamaguchi, K. *Chem. Phys. Lett.* **2003**, *374*, 45.

(5) (a) Lee, H. J.; Svahn, E.; Swanson, J. M. J.; Lepp, H.; Voth, G. A.; Brzezinski, P.; Gennis, R. B. *J. Am. Chem. Soc.* **2010**, *132*, 16225. (b) Näsvik Öjemyr, L.; Maréchal, A.; Vestin, H.; Meunier, B.; Rich, P. R.; Brzezinski, P. *Biochim. Biophys. Acta* **2014**, *1837*, 1012. (c) Kobayashi, K.; Tagawa, S.; Mogi, T. *J. Biochem.* **2009**, *145*, 685. (d) Rousseau, D. L.; Han, S.; Song, S.; Ching, Y.-C. *J. Raman Spectrosc.* **1992**, *23*, 551. (e) Belevich, I.; Borisov, V. B.; Konstantinov, A. A.; Verkhovsky, M. I. *FEBS Lett.* **2005**, *579*, 4567. (f) Babcock, G. T. *Proc. Natl. Acad. Sci. U.S.A.* **1999**, *96*, 12971.

(6) (a) Hosler, J.; Ferguson-Miller, S.; Calhoun, M.; Thomas, J.; Hill, J.; Lemieux, L.; Ma, J.; Georgiou, C.; Fetter, J.; Shapleigh, J.; Tecklenburg, M. J.; Babcock, G.; Gennis, R. *J. Bioenerg. Biomembr.* **1993**, *25*, 121. (b) Mogi, T.; Hirano, T.; Nakamura, H.; Anraku, Y.; Orii, Y. *FEBS Lett.* **1995**, *370*, 259. (c) Moody, A. J.; Mitchell, R.; Jeal, A. E.; Rich, P. R. *Biochem. J.* **1997**, *324*, 743.

(7) (a) Hematian, S.; Garcia-Bosch, I.; Karlin, K. D. *Acc. Chem. Res.* **2015**, *48*, 2462. (b) Rosenthal, J.; Nocera, D. G. *Acc. Chem. Res.* **2007**, *40*, 543. (c) Collman, J. P.; Boulatov, R.; Sunderland, C. J.; Fu, L. *Chem. Rev.* **2004**, *104*, 561. (d) Naruta, Y.; Sasaki, T.; Tani, F.; Tachi, Y.; Kawato, N.; Nakamura, N. *J. Inorg. Biochem.* **2001**, *83*, 239. (e) Baeg, J.-O.; Holm, R. H. *Chem. Commun.* **1998**, 571. (f) Lee, S. C.; Holm, R. H. *J. Am. Chem. Soc.* **1993**, *115*, 5833.

(8) (a) Lu, Y.; Yeung, N.; Sieracki, N.; Marshall, N. M. *Nature* **2009**, *460*, 855. (b) Yu, F.; Cangelosi, V. M.; Zastrow, M. L.; Tegoni, M.; Plegaria, J. S.; Tebo, A. G.; Mocny, C. S.; Ruckthong, L.; Qayyum, H.; Pecoraro, V. L. *Chem. Rev.* **2014**, *114*, 3495. (c) Farid, T. A.; Kodali, G.; Solomon, L. A.; Lichtenstein, B. R.; Sheehan, M. M.; Fry, B. A.; Bialas, C.; Ennist, N. M.; Siedlecki, J. A.; Zhao, Z.; Stetz, M. A.; Valentine, K. G.; Anderson, J. L. R.; Wand, A. J.; Discher, B. M.; Moser, C. C.; Dutton, P. L. *Nat. Chem. Biol.* **2013**, *9*, 826. (d) Gibney, B. R.; Tommos, C. *Photosystem II*; Springer: Berlin, 2005; p 729. (e) Ginovska-Pangovska, B.; Dutta, A.; Reback, M. L.; Linehan, J. C.; Shaw, W. J. *Acc. Chem. Res.* **2014**, *47*, 2621. (f) DeGrado, W. F.; Summa, C. M.; Pavone, V.; Nastri, F.; Lombardi, A. *Annu. Rev. Biochem.* **1999**, *68*, 779. (g) Antala, S.; Ovchinnikov, S.; Kamisetty, H.; Baker, D.; Dempski, R. E. *J. Biol. Chem.* **2015**, *290*, 17796.

(9) (a) Yeung, N.; Lin, Y.-W.; Gao, Y.-G.; Zhao, X.; Russell, B. S.; Lei, L.; Miner, K. D.; Robinson, H.; Lu, Y. *Nature* **2009**, *462*, 1079. (b) Lin, Y.-W.; Yeung, N.; Gao, Y.-G.; Miner, K. D.; Tian, S.; Robinson, H.; Lu, Y. *Proc. Natl. Acad. Sci. U.S.A.* **2010**, *107*, 8581. (c) Hayashi, T.; Miner, K. D.; Yeung, N.; Lin, Y.-W.; Lu, Y.; Moënne-Loccoz, P. *Biochemistry* **2011**, *50*, 5939. (d) Miner, K. D.; Mukherjee, A.; Gao, Y.-G.; Null, E. L.; Petrik, I. D.; Zhao, X.; Yeung, N.; Robinson, H.; Lu, Y. *Angew. Chem., Int. Ed.* **2012**, *51*, 5589. (e) Bhagi-Damodaran, A.; Petrik, I. D.; Marshall, N. M.; Robinson, H.; Lu, Y. *J. Am. Chem. Soc.* **2014**, *136*, 11882. (f) Chakraborty, S.; Reed, J.; Ross, M.; Nilges, M. J.; Petrik, I. D.; Ghosh, S.; Hammes-Schiffer, S.; Sage, J. T.; Zhang, Y.; Schulz, C. E.; Lu, Y. *Angew. Chem., Int. Ed.* **2014**, *53*, 2417. (g) Matsumura, H.; Hayashi, T.; Chakraborty, S.; Lu, Y.; Moënne-Loccoz, P. *J. Am. Chem. Soc.* **2014**, *136*, 2420. (h) Yu, Y.; Cui, C.; Liu, X.; Petrik, I. D.; Wang, J.; Lu, Y. *J. Am. Chem. Soc.* **2015**, *137*, 11570.

(10) (a) Davydov, R.; Hoffman, B. M. *Arch. Biochem. Biophys.* **2011**, *507*, 36. (b) Bollinger, J. M., Jr; Krebs, C. *J. Inorg. Biochem.* **2006**, *100*, 586. (c) Mbughuni, M. M.; Chakrabarti, M.; Hayden, J. A.; Bominaar, E. L.; Hendrich, M. P.; Münck, E.; Lipscomb, J. D. *Proc. Natl. Acad. Sci. U.S.A.* **2010**, *107*, 16788. (d) Astashkin, A. V.; Chen, L.; Elmore, B. O.; Kunwar, D.; Miao, Y.; Li, H.; Poulos, T. L.; Roman, L. J.; Feng, C. *J. Phys. Chem. A* **2015**, *119*, 6641. (e) Loewen, P. C.; Villanueva, J.; Switala, J.; Donald, L. J.; Ivancich, A. *Proteins: Struct., Funct., Genet.* **2015**, *83*, 853. (f) Symons, M. C. R.; Petersen, R. L. *Proc. R. Soc. London, Ser. B* **1978**, *201*, 285. (g) Davydov, R. M. *Biofizika* **1980**, *25*, 203. (h) Kappl, R.; Höhn-Berlage, M.; Hüttermann, J.; Bartlett, N.; Symons, M. C. R. *Biochim. Biophys. Acta* **1985**, *827*, 327. (i) Davydov, R.; Kofman, V.; Nocek, J. M.; Noble, R. W.; Hui, H.; Hoffman, B. M. *Biochemistry* **2004**, *43*, 6330. (j) Davydov, R.; Kofman, V.; Fujii, H.; Yoshida, T.; Ikeda-Saito, M.; Hoffman, B. M. *J. Am. Chem. Soc.* **2002**, *124*, 1798. (k) Davydov, R.; Laryukhin, M.; Ledbetter-Rogers, A.; Sono, M.; Dawson, J. H.; Hoffman, B. M. *Biochemistry* **2014**, *53*, 4894. (l) Davydov, R.; Makris, T. M.; Kofman, V.; Werst, D. E.; Sligar, S. G.; Hoffman, B. M. *J. Am. Chem. Soc.* **2001**, *123*, 1403. (m) Davydov, R.; Macdonald, I. D. G.; Makris, T. M.; Sligar, S. G.; Hoffman, B. M. *J. Am. Chem. Soc.* **1999**, *121*, 10654. (n) Davydov, R. M.; Chauhan, N.; Thackray, S. J.; Anderson, J. L. R.; Papadopoulou, N. D.; Mowat, C. G.; Chapman, S. K.; Raven, E. L.; Hoffman, B. M. *J. Am. Chem. Soc.* **2010**, *132*, 5494. (o) Davydov, R.; Razeghifard, R.; Im, S.-C.; Waskell, L.; Hoffman, B. M. *Biochemistry* **2008**, *47*, 9661.

(11) Denisov, I. G. *Physical Inorganic Chemistry*; John Wiley & Sons, Inc.: New York, 2010; p 109.

(12) (a) Davydov, R.; Gilep, A. A.; Strushkevich, N. V.; Usanov, S. A.; Hoffman, B. M. *J. Am. Chem. Soc.* **2012**, *134*, 17149. (b) Davydov, R.; Matsui, T.; Fujii, H.; Ikeda-Saito, M.; Hoffman, B. M. *J. Am. Chem. Soc.* **2003**, *125*, 16208. (c) Davydov, R.; Osborne, R. L.; Kim, S. H.; Dawson, J. H.; Hoffman, B. M. *Biochemistry* **2008**, *47*, 5147.

(13) As reported previously,[10g,h] formation of the $g = 2.32$ hydroperoxo species upon annealing at $T \geq 190$ K results from protonation by His64.

(14) Unno, M.; Chen, H.; Kusama, S.; Shaik, S.; Ikeda-Saito, M. *J. Am. Chem. Soc.* **2007**, *129*, 13394.

(15) X-ray irradiation during data collection is known to result in cryoreduction of oxy-heme to (hydro)peroxo.[14] The resolution of 5HAV is not high enough to observe the change of the O−O ligand associated with this reduction. Regardless of whether the dioxygen is oxy or (hydro)peroxo, this structure supports our key finding: the presence of an extended H-bond network engaging the bound O−O ligand.

(16) Vojtěchovský, J.; Chu, K.; Berendzen, J.; Sweet, R. M.; Schlichting, I. *Biophys. J.* **1999**, *77*, 2153.

(17) (a) Denisov, I. G.; Sligar, S. G. In *Cytochrome P450*; Ortiz de Montellano, P. R., Ed.; Springer: Berlin, 2015; p 69. (b) Nagano, S.; Poulos, T. L. *J. Biol. Chem.* **2005**, *280*, 31659. (c) Zhao, B.; Guengerich, F. P.; Voehler, M.; Waterman, M. R. *J. Biol. Chem.* **2005**, *280*, 42188. (d) Schlichting, I.; Berendzen, J.; Chu, K.; Stock, A. M.; Maves, S. A.; Benson, D. E.; Sweet, R. M.; Ringe, D.; Petsko, G. A.; Sligar, S. G. *Science* **2000**, *287*, 1615.

DOI: 10.1021/jacs.5b12004
J. Am. Chem. Soc. 2016, 138, 1134−1137